Letter

Nonequilibrium dynamical behavior in noncoplanar magnets with chiral spin texture

Takayuki Shiino,[1,*] Fernand Denoel,[1] Girma Hailu Gebresenbut,[2] Cesar Pay Gómez,[2] Per Nordblad,[1] and Roland Mathieu[1,†]
[1]*Department of Materials Science and Engineering, Uppsala University, Box 35, 751 03 Uppsala, Sweden*
[2]*Department of Chemistry, Ångström Laboratory, Structural Chemistry, Uppsala University, 751 21 Uppsala, Sweden*

(Received 28 February 2022; accepted 4 May 2022; published 16 May 2022)

We observe nonequilibrium dynamical magnetic behavior in the magnetically ordered phase of a Tsai-type Tb-Au-Si quasicrystal approximant system. The magnetic texture in the ordered phase is found to exhibit scalar spin chirality (SSC) order, inferring that SSC is the order parameter of the present magnetic system. We further find that the introduction of "pseudo-Tsai" clusters, associated with additional Tb atoms in the structure, induces spin-glass dynamics. We discuss the observed dynamical magnetic behavior in the Tb-Au-Si systems, considering the effect of the pseudo-Tsai clusters on the magnetic configuration and local spin chirality.

DOI: 10.1103/PhysRevB.105.L180409

Spin glasses (SGs) have been a central topic in physics due to their intriguing nonequilibrium dynamics and their application to information science and technology [1–4]. The influence of SGs on condensed matter physics is diverse as glassy behavior has been investigated not only in archetypal disordered systems, but also in various complex systems [5,6], including geometrically frustrated magnetic systems [7], chiral-glass superconductors [8], orientational glasses [9], and supercooled liquids [10]. Experimentally, e.g., by magnetometry, SGs are found to display aging, memory, and rejuvenation features [11,12]. Aging refers to the rearrangement or slow equilibration of the random spin configuration imprinted to the system after, e.g., a temperature perturbation (rapid cooling into the SG phase), while memory and rejuvenation depict the ability of the SG phase to both preserve this aging (memory) and reinitialize its spin configuration (rejuvenation = "young" anew) after subsequent perturbations.

Magnetic quasicrystals (QCs) and their approximant crystals (ACs) [13] are promising new playgrounds for SG and frustration magnetism due to their unique geometrical structure [14]. In particular, rare-earth (RE)-contained Tsai-type 1/1 ACs [13] are of interest due to their unique polyhedral structures [15]. There are two possible views for the network of the magnetic RE sites (see Fig. 1): either by a periodic arrangement of magnetic icosahedral units [16] or by distorted corner-sharing octahedral units [14,17], both of which consist of triangular faces (and thus geometrical frustration is expected). Interestingly, noncoplanar spiral-like magnetic order has been observed in the Tb-Au-Si 1/1 AC [18–20] and Ho-Au-Si 1/1 AC [20].

*neomi.taka.shin@gmail.com
†roland.mathieu@angstrom.uu.se

In this Letter, we investigate magnetic nonequilibrium dynamics of the Tb-Au-Si (TAS) 1/1 AC systems. We investigate three compositionally different systems named TAS(0), TAS(14), and TAS(100). The number in the parentheses indicates the percentage of "pseudo-Tsai" clusters [15], which gives additional RE atoms at the center of the icosahedral shells as illustrated in Fig. 1(a). Based on our previous neutron-scattering data (temperature $T = 2$ K) reported in Ref. [20], we first discuss the order of the scalar spin chirality (SSC) in the magnetically ordered phase of TAS(0). We find that the ac susceptibility of the TAS exhibits relaxation behavior at constant T below the ordering temperatures. We further observe "aging," "rejuvenation," and "memory" effects in the dc magnetization and ac susceptibility of the pseudo-Tsai TAS systems [i.e., TAS(14) and TAS(100)]. On the other hand, TAS(0) exhibits no memory effect, but a peculiar cooling-history-dependent behavior in its dc magnetization. These results indicate that TAS(0), which can be considered a magnetically frustrated ferrimagnet with chiral spin texture, is at the border of becoming a SG. We discuss the origin of the nonequilibrium dynamics in light of the introduction of pseudo-Tsai clusters and the chiral spin texture of the system.

We have used the same polycrystalline samples as in our previous studies: see Refs. [15,20] for details about the synthesis conditions and characterizations (note that in Ref. [15], the 0 and 100 systems are referred to as IT and CC, respectively). The dc magnetization and ac magnetic susceptibility measurements were performed using an MPMS XL superconducting quantum interference device (SQUID) magnetometer (Quantum Design Inc.). The Hall effect was measured using a conventional four-probe method in a Physical Property Measurement System (PPMS) (Quantum Design Inc.).

The local SSC and vector spin chirality (VSC) for each triangular unit (see Fig. 1) are defined by $\chi_{ijk} = \vec{S}_i \cdot (\vec{S}_j \times \vec{S}_k)$ and $\vec{\chi}_{ijk} = \vec{S}_i \times \vec{S}_j + \vec{S}_j \times \vec{S}_k + \vec{S}_k \times \vec{S}_i$, respectively, where $\vec{S}_i$, $\vec{S}_j$, and $\vec{S}_k$ are spins residing on the vertices in the counterclockwise order of $i \to j \to k$ (cyclic). In the octahedral spin configuration of TAS(0) ($T = 2$ K), presented in Fig. 1(b) and its schematic expanded view in Fig. 1(c), the

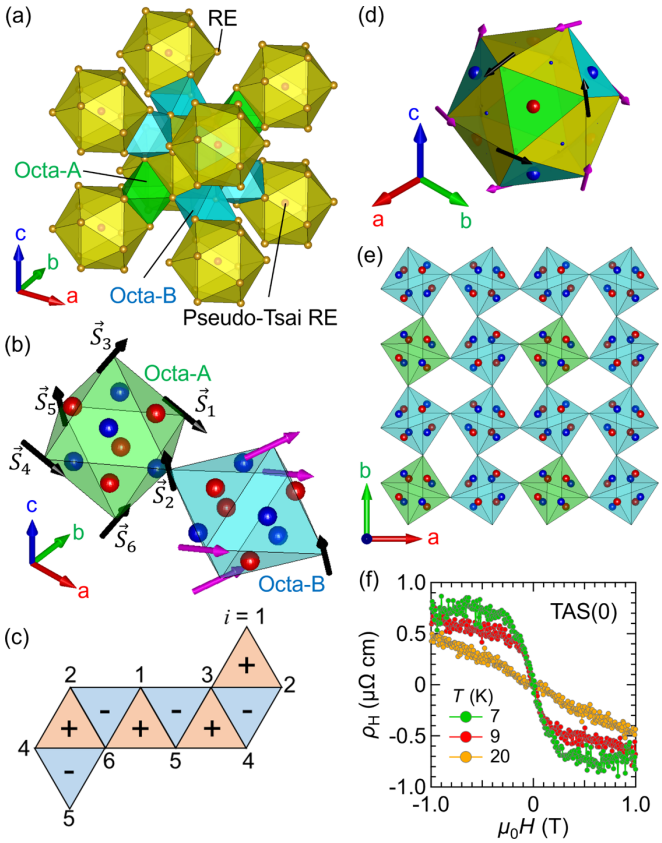

FIG. 1. (a) Body-centered periodic arrangement of RE (=Tb) icosahedra (yellow) and pseudo-Tsai RE atoms. The interstitial (distorted) octahedral units named Octa-A (green) and Octa-B (blue) are also presented. (b) The spin configuration on the octahedra of TAS(0) obtained from the previous neutron-scattering experiment [20]. The black and pink arrows (spins) refer to two independent moments RE1_1 and RE1_2, respectively [20]. The SSC is indicated by the red and blue spheres whose size and color represent the absolute value and sign, respectively. (c) A schematic expanded view of the octahedral unit. The sign (±) indicates the sign of SSC. (d) The spin configuration on the icosahedral unit of TAS(0) with the SSC representations. The green and blue faces are shared with the octahedral units Octa-A and Octa-B, respectively. (e) The periodic arrangement of the octahedral units exhibiting the SSC in the ordered phase of TAS(0). (f) The Hall resistivity of TAS(0) measured below and above the ordering temperature ($T_m \approx 11$ K).

(i, j, k) combinations for local SSC and VSC are $(i, j, k) = (1, 3, 2)$, $(2, 3, 4)$, $(3, 5, 4)$, $(1, 5, 3)$, $(1, 6, 5)$, $(1, 2, 6)$, $(2, 4, 6)$, and (4,5,6). In Fig. 1(b), the calculated values of SSC are indicated by color spheres at the center of the triangular faces: the size of the sphere represents the absolute value of SSC, while the color indicates the sign of SSC (red: +, blue: −). The sign of SSC alternates between two neighboring triangular faces sharing an edge, as is also presented in Fig. 1(c). The total SSC of the octahedral unit ($\chi_{\rm octa}$) can be described as $\chi_{\rm octa} = (\vec{S}_3 - \vec{S}_6) \cdot [(\vec{S}_1 - \vec{S}_4) \times (\vec{S}_2 - \vec{S}_5)]$ and $\chi_{\rm octa}$ is zero since $\vec{S}_i = \vec{S}_{i+3}$ ($i = 1$, 2, and 3) in the present spin configuration. From the icosahedral point of view, only the triangular faces shared with the octahedra exhibit significant finite values of SSC [see Fig. 1(d)]. This suggests that the octahedral network is more relevant to the chirality of the present system. We also observe that the VSC of the octahedra tends to point along the [111] (threefold) direction in parallel and antiparallel (see the Supplemental Material (SM) [21], which includes Ref. [22]). Figure 1(e) shows the periodic arrangement of the octahedral units with the SSC representations. Note that there are two different types of spin octahedra, named Octa-A (green) and Octa-B (blue). The former consists of only one type of moment, referred to as RE1_1 (black), while the latter consists of two types of moments, RE1_1 and RE1_2 (pink) [20]. The Octa-A octahedra contain an inherent threefold axis, while Octa-B octahedra do not. None of the octahedra exhibit full cubic symmetry. Yet, interestingly, their SSC absolute values are only slightly different (by ∼1%), and we observe a periodic order with respect to the SSC (the sign of the SSC is alternating in space). This indicates that TAS(0) is a chiral order system regarding its octahedral network. Furthermore, we observe an anomalous Hall effect (AHE) below the magnetic ordering temperature (∼11 K) (see Fig. 1(f) and SM [21]). The magnetotransport and AHE of such systems may include contributions of the chiral order.

In neutron-diffraction experiments, the TAS systems appear as long-range ferrimagnets [20]. Magnetic-field-dependent magnetization curves recorded at low temperatures support this observation [15]. However the temperature-dependent magnetization curves suggest differences between the TAS systems. Figures 2(a)–2(c) show the temperature dependence of the dc magnetization [plotted as M/H for zero field cooling (ZFC) and field cooling (FC)] and ac magnetic susceptibility (the in-phase χ' and out-of-phase χ'' components) of the TAS systems [see SM [21] for a comparison of $M(T)/H$ and $\chi'(T)$]. The ZFC magnetization exhibits a maximum (at T_m) below which irreversibility is observed between the ZFC and FC curves, indicating ferrimagnetic ordering below T_m. The TAS(14) and TAS(100) systems display frequency-dependent onsets of χ'' [see Figs. 2(b) and 2(c)], which are reminiscent of those observed in SGs [23]. Additional data on a wider frequency range were collected in order to perform a dynamic scaling analysis and evidence SG phase transitions in those two systems (see SM [21]). The results are, however, not completely satisfactory. For information, if we consider a SG transition temperature $T_g \sim T_m \sim 7$ K for TAS(100), and the critical slowing down relation $\tau/\tau_0 = [(T - T_g)/T_g]^{-z\nu}$ for the relaxation time τ [24], a value of the $z\nu$ exponent of 6 and $\tau_0 \sim 10^{-9}$ s are obtained (see SM [21]).

Figures 2(d)–2(f) show the time dependence of the out-of-phase component of the ac susceptibility χ''. Note that the first point ($t = 0$) was recorded after rapidly cooling the systems from $T = 20$ K (above T_m) to the measurement temperature. In the ac experiments, an ac excitation with a given frequency f is used to probe the magnetic response. The ac frequency will set the observation time of the measurement as $t_{\rm obs} \sim 1/(2\pi f)$. We observe clear time relaxation and decay of χ'' (and χ') below T_m, indicating glassylike nonequilibrium dynamics [11,25] below T_m, even for TAS(0) whose temperature-dependent dc magnetization and ac susceptibility suggest a regular long-range ferrimagnet order [Figs. 2(a)–2(c)]. The relaxation is smaller at lower temperatures for all systems, yet it vanishes below 5 K in the case of TAS(0), suggesting some differences between TAS(0) and the two other systems.

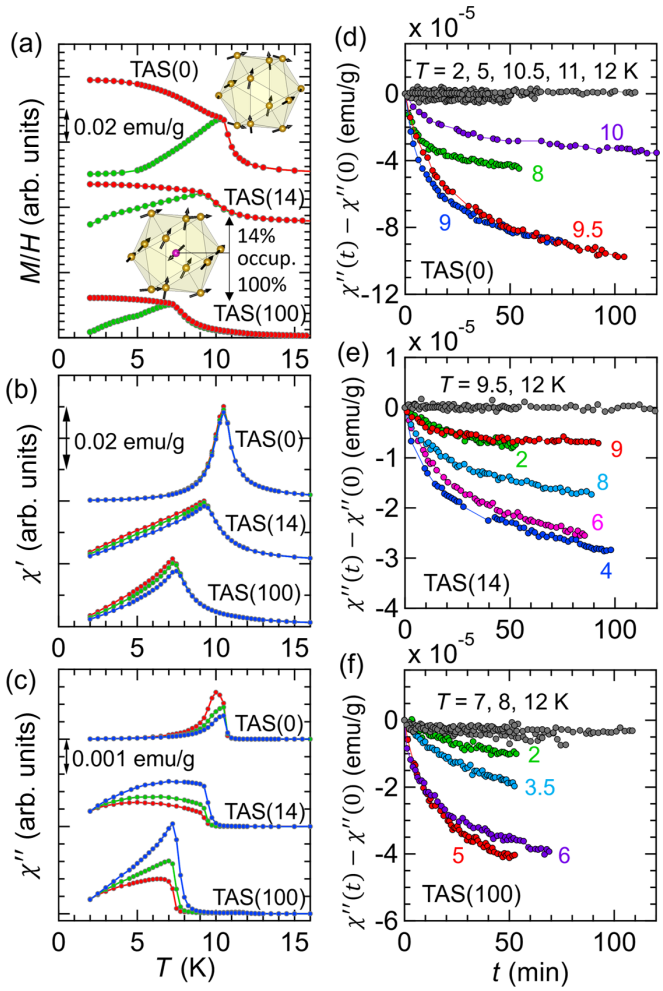

FIG. 2. (a) The ZFC (green) and FC (red) magnetization M (plotted as M/H) recorded under a magnetic field of $H = 10$ Oe. (b),(c) The in-phase (χ') and out-of-phase (χ'') components of the ac magnetic susceptibility, respectively. The data curves in (a)–(c) are arbitrarily shifted from the origin. The ac susceptibility was recorded using the ac excitation $h = 4$ Oe at frequencies $f = 1.7$ (red), 17 (green), and 170 Hz (blue). The data presented for (a)–(c) are from Refs. [15,20]: note that we remeasured the magnetization for TAS(0) in this study. The schematics in (a) illustrate Tsai-type [TAS(0)] and pseudo-Tsai-type [TAS(14) and TAS(100)] RE clusters. (d)–(f) Time dependence of χ'' for (d) TAS(0), (e) TAS(14), and (f) TAS(100) at several temperatures, which was recorded with $h = 4$ Oe and $f = 1.7$ Hz.

Another interesting property of the SG phase is that it may both remember and forget the aging which occurred at a given temperature, yielding the observed memory (i.e., the system remember its "age") and rejuvenation (i.e., the system instead appears "younger") phenomena [23] owing to the chaotic nature of the glassy phase (temperature chaos [26]). The aging which took place during a halt at a given temperature will not affect the spin configuration at a lower temperature, outside a temperature range set by an overlap length of the equilibrium configurations [23], implying that the system appears younger when reaching that temperature (rejuvenation) [26]. However, the configuration established at the initial temperature is preserved and is retrieved if the temperature is set back to that temperature (memory). Such memory and rejuvenation effects may be probed in time-dependent measurements [23,26], but also in temperature-dependent ones, yielding so-called memory dips [11,26].

The dc and ac memory experiments [11,26] are hence performed on all systems. In both the dc and ac cases, the sample is rapidly cooled in zero magnetic field below T_m down to the halt temperature T_{halt}, where the cooling is stopped for a given halt time t_{halt}. The cooling is then resumed down to 2 K and the magnetization or ac susceptibility is recorded on reheating and compared to that obtained without halt during the cooling. In the dc measurements, a small magnetic field is applied at 2 K before recording the magnetization on reheating (i.e., the obtained magnetization curves are zero-field-cooled curves). In the ac ones, it is possible to record the susceptibility while cooling the sample, as well as during the halt and its subsequent cooling. As aging proceeds while the ac susceptibility is being collected, reference curves measured without halt during the cooling, both for cooling and subsequent reheating, need to be acquired [23]. The effect of the halt is visualized more easily in the difference plots of the aging/memory curves with their corresponding references [$\Delta M(T)$ or $\Delta\chi'(T)$]. In both ac and dc experiments, the amplitude of the ac excitation and dc magnetic field is small enough not to disturb a linear response down to the ordering temperature (see SM [21]).

The results of dc-memory experiments are shown in Figs. 3(a)–3(c). Note that $\Delta M = M(t_{halt} \neq 0) - M(t_{halt} = 0)$, where M is the ZFC dc magnetization. See the SM [21] for the $M(T)$ data obtained after different t_{halt}. TAS(14) and TAS(100) show the characteristic memory dips of the depth increasing with increasing halt time, centered at T_{halt} [12]. For TAS(0), however, the observed dips are not centered at T_{halt}, but reflect instead the frequency dependence of the ac susceptibility, which is observed between T_m and ~5 K [see Fig. 2(c)]. This suggests that the observed dips reflect the effective cooling rate of the experiment [27], rather than the memory of the aging. This was confirmed by recording reference zero-field-cooled magnetization curves (without halt) after cooling at different cooling rates—mimicking the results observed for "memory" experiments with different t_{halt} (see SM [21]).

Figures 3(d)–3(f) show the results of ac-memory effect measurements. Note that $\Delta\chi'' = \chi''(t_{halt} \neq 0) - \chi''(t_{halt} = 0)$, where the cooling and warming references $\chi''(t_{halt} = 0)$ are obtained for aging and memory measurements, respectively. As in the dc experiments, the memory effect (red curves) is observed in TAS(14) and TAS(100). However, memory behavior is absent in TAS(0), and there is no memory dip at T_{halt}, as shown in Fig. 3(d). This is reminiscent of frustrated (ferro- or ferri)magnets [28] or the ferro-/ferrimagnetic phase of reentrant ferromagnets [29], which display aging, yet whose magnetic configuration is unstable to any temperature perturbation, even when cooling to a lower temperature, and no memory in observed in that phase [29].

Interestingly, the reference warming $\chi''(T)$ curves for the TAS systems are slightly below their reference cooling curves [see the insets of Figs. 3(d)–3(f)]. This suggests that the aging which takes places during the cooling proceeds during the subsequent reheating, and thus that the aging is accumulative

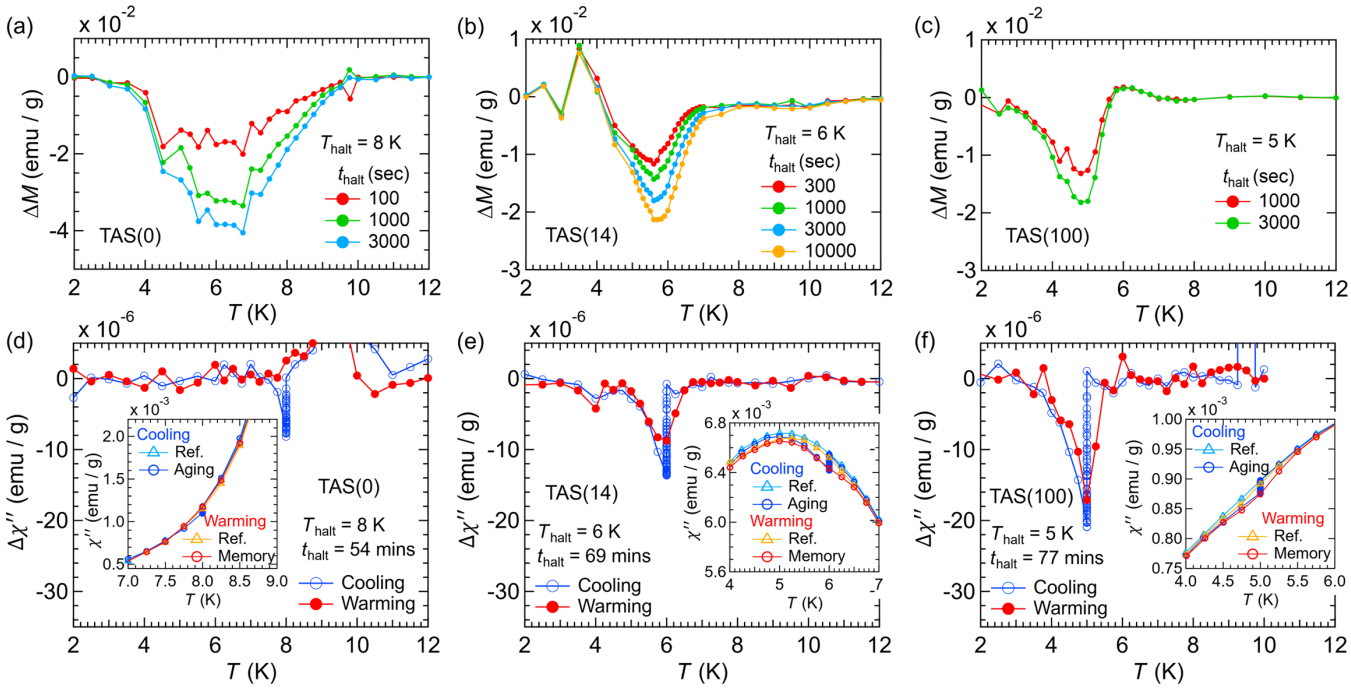

FIG. 3. (a)–(c) The results of the dc memory measurements: ΔM vs temperature, where $\Delta M = M(t_{\rm halt} \neq 0) - M(t_{\rm halt} = 0)$. (d)–(f) The results of the ac memory measurements: $\Delta\chi''$ vs temperature, where $\Delta\chi'' = \chi''(t_{\rm halt} \neq 0) - \chi''(t_{\rm halt} = 0)$. The inset shows χ'' vs temperature for the aging (in the cooling process) and memory (in the warming process) measurements at $T_{\rm halt}$. Note that the reference curves $[\chi''(t_{\rm halt} = 0)]$ are obtained both in the cooling process (for the reference of the aging curve) and the warming process (for the reference of the memory curve).

in character [23]. This is qualitatively similar to that observed for Ising SG, in contrast to Heisenberg ones in which the aging is not accumulative and the reheating curve lies above the cooling one [23]. This is in agreement with the results of the memory experiments, as the memory dips observed for TAS(14) and TAS(100) are rather broad (see SM [21] for dc ones) as for Ising SGs, again owing to the accumulative/less chaotic nature of the aging.

Our three TAS systems exhibit low-temperature $M(H)$ curves resembling those of ferrimagnets (see SM [21]), although only TAS(0) shows $M(T)$ and $\chi(T)$, suggesting long-range order (sharp, frequency-independent onset of magnetic ordering; see Figs. 2(a)–2(c) and Fig. S3 in SM [21]); interestingly, TAS(0) also shows chiral order. Spin-glass behavior is induced by the introduction of pseudo-Tsai RE atoms as in TAS(14) and TAS(100), possibly owing to a larger randomness and magnetic frustration or perturbation of the chiral spin texture and chiral order. We have observed a similar behavior of χ'' with time for the related Ho-Au-Si system [20] (see SM [21]; onsets of magnetic order in that system are, however, too low to perform temperature-dependent memory experiments), suggesting that the spin/chiral states and their evolution upon the introduction of a pseudo-Tsai RE atom are a general feature of these approximant crystals. It is interesting to mention in this glassy context that in the chirality scenario of the SG ordering (chiral glass) proposed by Kawamura [5,30], the chirality of spins is a hidden order parameter of the SG transition and the chirality may order independently or can be coupled to the spins in the presence of weak random anisotropy; the ordering of chirality induces the spin (glass) order.

In conclusion, we have observed nonequilibrium dynamical behavior in seemingly long-range systems, the base system of which [i.e., TAS(0)] exhibits the order of SSC on its octahedral spin network. The pseudo-Tsai systems [i.e., TAS(14) and TAS(100)] exhibit SG features as confirmed by memory effects, while TAS(0) exhibits no memory but peculiar nonequilibrium behavior that depends on the cooling history, akin to a frustrated ferrimagnet. We hope that our findings stimulate the studies of the dynamical magnetic properties and magnetotransport/AHE in this class of systems.

We thank the Knut and Alice Wallenberg Foundation (Grant No. KAW 2018.0019), the Carl Tryggers Stiftelse för Vetenskaplig Forskning (Grant No. CTS 19:235), and the Swedish Research Council (VR).

[1] M. Mezard, G. Parisi, and M. Virasoro, *Spin Glass Theory and Beyond* (World Scientific, Singapore, 1986).

[2] D. S. Fisher and D. A. Huse, Nonequilibrium dynamics of spin glasses, Phys. Rev. B **38**, 373 (1988).

[3] D. S. Fisher and D. A. Huse, Equilibrium behavior of the spin-glass ordered phase, Phys. Rev. B **38**, 386 (1988).

[4] A. J. Bray and M. A. Moore, Chaotic Nature of the Spin-Glass Phase, Phys. Rev. Lett. **58**, 57 (1987).

[5] H. Kawamura and T. Taniguchi, in *Spin Glasses* (Elsevier Science, Amsterdam, 2015), Chap. 1, pp. 1–137.

[6] P. Nordblad, Competing interaction in magnets: The root of ordered disorder or only frustration?, Phys. Scr. **88**, 058301 (2013).

[7] V. Dupuis, E. Vincent, J. Hammann, J. E. Greedan, and A. S. Wills, Aging and memory properties of topologically frustrated magnets, J. Appl. Phys. **91**, 8384 (2002).

[8] A. Gardchareon, R. Mathieu, P. E. Jönsson, and P. Nordblad, Strong rejuvenation in a chiral-glass superconductor, Phys. Rev. B **67**, 052505 (2003).

[9] F. Alberici-Kious, J. P. Bouchaud, L. F. Cugliandolo, P. Doussineau, and A. Levelut, Aging in $K_{1-x}Li_xTaO_3$: A Domain Growth Interpretation, Phys. Rev. Lett. **81**, 4987 (1998).

[10] R. L. Leheny and S. R. Nagel, Frequency-domain study of physical aging in a simple liquid, Phys. Rev. B **57**, 5154 (1998).

[11] K. Jonason, E. Vincent, J. Hammann, J. P. Bouchaud, and P. Nordblad, Memory and Chaos Effects in Spin Glasses, Phys. Rev. Lett. **81**, 3243 (1998).

[12] R. Mathieu, P. Jönsson, D. N. H. Nam, and P. Nordblad, Memory and superposition in a spin glass, Phys. Rev. B **63**, 092401 (2001).

[13] T. Fujiwara and Y. Ishii, *Quasicrystals* (Elsevier Science, Amsterdam, 2007), Vol. 3.

[14] T. Shiino, F. Denoel, G. H. Gebresenbut, D. C. Joshi, Y.-C. Huang, C. P. Gómez, U. Häussermann, A. Rydh, and R. Mathieu, Singular magnetic dilution behavior in a quasicrystal approximant, Phys. Rev. B **104**, 224411 (2021).

[15] G. Gebresenbut, T. Shiino, D. Eklöf, D. C. Joshi, F. Denoel, R. Mathieu, U. Häussermann, and C. Pay Gómez, Atomic-Scale Tuning of Tsai-Type Clusters in RE–Au–Si Systems (RE = Gd, Tb, Ho), Inorg. Chem. **59**, 9152 (2020).

[16] P. Koželj, S. Jazbec, S. Vrtnik, A. Jelen, J. Dolinšek, M. Jagodič, Z. Jagličić, P. Boulet, M. C. de Weerd, J. Ledieu, J. M. Dubois, and V. Fournée, Geometrically frustrated magnetism of spins on icosahedral clusters: The $Gd_3Au_{13}Sn_4$ quasicrystalline approximant, Phys. Rev. B **88**, 214202 (2013).

[17] M. G. Kim, G. Beutier, A. Kreyssig, T. Hiroto, T. Yamada, J. W. Kim, M. de Boissieu, R. Tamura, and A. I. Goldman, Antiferromagnetic order in the quasicrystal approximant Cd_6Tb studied by x-ray resonant magnetic scattering, Phys. Rev. B **85**, 134442 (2012).

[18] T. J. Sato, A. Ishikawa, A. Sakurai, M. Hattori, M. Avdeev, and R. Tamura, Whirling spin order in the quasicrystal approximant $Au_{72}Al_{14}Tb_{14}$, Phys. Rev. B **100**, 054417 (2019).

[19] T. Hiroto, T. J. Sato, H. Cao, T. Hawai, T. Yokoo, S. Itoh, and R. Tamura, Noncoplanar ferrimagnetism and local crystalline-electric-field anisotropy in the quasicrystal approximant $Au_{70}Si_{17}Tb_{13}$, J. Phys.: Condens. Matter **32**, 415802 (2020).

[20] G. H. Gebresenbut *et al.*, Effect of pseudo-Tsai cluster incorporation on the magnetic structures of RE-Au-Si (RE = Tb, Ho) Quasicrystal Approximants (unpublished).

[21] See Supplemental Material at http://link.aps.org/supplemental/10.1103/PhysRevB.105.L180409 for details about VSC, AHE, comparison of dc magnetization and ac susceptibility, scaling analysis on the SG behavior, dc memory, M vs H curves, and the magnetic property of Ho-Au-Si.

[22] D. C. Joshi, G. Gebresenbut, C. Pay Gomez, and R. Mathieu, Memory and rejuvenation in a quasicrystal, Europhys. Lett. **132**, 27002 (2020).

[23] P. E. Jönsson, R. Mathieu, P. Nordblad, H. Yoshino, H. A. Katori, and A. Ito, Nonequilibrium dynamics of spin glasses: Examination of the ghost domain scenario, Phys. Rev. B **70**, 174402 (2004).

[24] P. C. Hohenberg and B. I. Halperin, Theory of dynamic critical phenomena, Rev. Mod. Phys. **49**, 435 (1977).

[25] R. Mathieu, D. Akahoshi, A. Asamitsu, Y. Tomioka, and Y. Tokura, Colossal Magnetoresistance without Phase Separation: Disorder-Induced Spin Glass State and Nanometer Scale Orbital-Charge Correlation in Half Doped Manganites, Phys. Rev. Lett. **93**, 227202 (2004).

[26] R. Mathieu, P. E. Jönsson, P. Nordblad, H. A. Katori, and A. Ito, Memory and chaos in an Ising spin glass, Phys. Rev. B **65**, 012411 (2001).

[27] E. Vincent, Ageing, rejuvenation and memory: The example of spin glasses, Lect. Notes Phys. **716**, 7 (2007).

[28] D. N. H. Nam, R. Mathieu, P. Nordblad, N. V. Khiem, and N. X. Phuc, Ferromagnetism and frustration in $Nd_{0.7}Sr_{0.3}MnO_3$, Phys. Rev. B **62**, 1027 (2000).

[29] K. Jonason and P. Nordblad, Sensitivity to temperature perturbations of the ageing states in a re-entrant ferromagnet, Eur. Phys. J. B **10**, 23 (1999).

[30] H. Kawamura, Chirality scenario of the spin-glass ordering, J. Phys. Soc. Jpn. **79**, 011007 (2010).